SEMARAK ILMU
PUBLISHING
202103268166(003316878-P)

Journal of Advanced Research in Fluid
Mechanics and Thermal Sciences

Journal homepage:
https://semarakilmu.com.my/journals/index.php/fluid_mechanics_thermal_sciences/index
ISSN: 2289-7879

Numerical Simulation of Laser Soldering Process on Pin Through Hole (PTH)

Saifulmajdy A. Zahiri[1], Mohamad Aizat Abas[1,*], Fei Chong Ng[1], Mohamad Fikri Mohd Sharif[2], Fakhrozi Che Ani[2]

[1] School of Mechanical Engineering, Universiti Sains Malaysia, Engineering Campus, Nibong Tebal, 14300, Penang, Malaysia
[2] Western Digital, MK13, Plot 301A Persiaran Cassia Selatan 1 Taman Perindustrian, Batu Kawan, 14100, Penang, Malaysia

ARTICLE INFO

Article history:
Received 10 March 2022
Received in revised form 25 June 2022
Accepted 5 July 2022
Available online 30 July 2022

Keywords:
Computational Fluid Dynamics (CFD); laser soldering; Pin Through Hole (PTH); Finite Volume Method (FVM); lead-free solder; SAC 305

ABSTRACT

The increasing demands in the miniaturization of microelectronic products promotes the automation of electronic assembly and manufacturing process such as laser soldering to deliver high quality and flexibility of solder joints. This paper investigates possibility of using computational fluid dynamics (CFD) to create simulation of laser soldering process. Heating process of solder phase was simulated Using finite volume method (FVM) and energy equation enabled. Results of the simulation was compared with experiment for validation. Generally, it is found that the solder formation is identical for both simulation and experimental process. Moreover, the temperature distribution shows that heating process of laser soldering has great heating distribution along the solder region.

1. Introduction

Recently, in microelectronic and optoelectronic industry, production of miniature electronic devices and the use of temperature sensitive components are increasing. The fabrication of this devices has become extremely complex and harder to produce a quality product with high repeatability. This led to new, highly precise integration process of electronic part such as laser soldering technology. The laser is specially used for soldering of the temperature sensitive assemblies and it is also used in joining of assemblies with high thermal capacity that could not be conventionally soldered in the reflow process [1].

Laser soldering is a process where a precisely focused laser beam provides controlled heating of the solder alloy leading to a fast and non-destructive solder joint. The process uses a controlled laser beam to radiate energy to a soldering location where the absorbed energy heats the solder until it reaches its melting temperature [2]. The melted solder spread to the contact surface of solder region and bind the two adjacent surfaces. This heating process completely eliminates any mechanical contact from the heat source.

---

[*] *Corresponding author.*
E-mail address: aizatabas@usm.my

https://doi.org/10.37934/arfmts.98.1.137145

The reliability and quality of solder joints may be influenced by the characterization of solder materials and its filling of molten solder in PCB holes. Leaded-based solder materials are hazardous and not environment friendly. The use of certain material elements is forbidden by the European Union Restriction of Hazardous Substances [3,4]. Thus, lead-free solder materials are introduced in the application of soldering in electronic packaging assemblies. Furthermore, the use of nitrogen can increase the performance of using lead-free solder material in the manufacturing industry [4]. However, due to higher temperature required to melt lead free solder, silver content higher than 2% in lead free solder will induce stresses in assembly due to high mismatch in the coefficient of thermal expansion (CTE) [5]. In this case, laser soldering can overcome this issue by manipulating laser power and duration of the laser beam to prevent unnecessary long exposure of the solder to heat.

In previous research, finite element analysis (FEA) that are involved in prediction the failure of solder joints by simulation methods [4,6,7]. However, this research mainly focuses on reliability of solder joints in other soldering processes. In addition, there is no research being done on the optimization of laser soldering parameters on passive devices. This could be ideally considered to increase the quality of solder joints in the laser soldering process. Furthermore, numerical simulation results cannot be completely taken as a result because it must be verified by experimental or calculation method [8]. This is because comparison is required to verify the validity of this study to know the range of the results. The numerical analysis results are essential for better understanding of relevant researchers and engineers in the electronic industry [9].

Solder joint reliability is the most imperative aspect in the process quality of re-flow soldering. However, a major issue in laser soldering is the wetting ability of the solder to secure the joint. In addition, visualization of the molten filling process is difficult because of the small pin-through-hole (PTH) size, and investigations on laser soldering using computational fluid dynamics (CFD) are still limited. Thus, this topic was considered in the current study to investigate the effects of laser heating temperature using the CFD modeling approach. As mentioned above, the molten solder material is heated by laser beam during laser soldering. Thus, the modeling in this study should consider and enable the heating effect during laser soldering. In this study, the energy equation was considered in the CFD simulation. The outcomes of the study are expected to enhance the understanding of geometrical positioning with detailed visualization of laser soldering. The molten solder profile driven by heating action is compared with the experimental result.

2. Methodology

This section detailed the numerical simulation of laser soldering process on a pin to hole (PTH) assembly. In this numerical work, the commercially available finite volume method (FVM) based software, ANSYS Fluent was used.

The present numerical simulation work was governed by the Navier-Stokes equation, which included the continuity equation, momentum equation and energy equation, respectively given as follows

$$\frac{\partial \rho}{\partial t} + \nabla.(\rho \vec{u}) = 0, \tag{1}$$

$$\frac{\partial}{\partial t}(\rho \vec{u}) + \nabla \cdot (\rho\, \vec{u} \cdot \vec{u}) = -\nabla p + \nabla \vec{\tau} + \rho \vec{g}, \tag{2}$$

$$\rho C_P \left(\frac{\partial T}{\partial t} + \vec{u} \nabla T\right) = \nabla(k \nabla T) + \Phi, \tag{3}$$

where ρ denotes the density of the fluid, $\vec{u}$ is the fluid flow velocity, C_p is the specific heat capacity, T is the temperature, k is the thermal conductivity, Φ is the heat flux, $\vec{\tau}$ is the shear stress and gravitational acceleration, $\vec{g}$. The model is based on two phase interactions of SAC 305 solder and air. To track the flow front of SAC305 solder, the multiphase volume of fluid (VOF) model was employed. The volume fraction of SAC305 solder phase, f lies in the range of 0 to 1, with the unity value of f implying the presence of SAC 305 solder. The VOF model was governed by the transport equation given as follows

$$\frac{\partial f}{\partial t} + \vec{u} \cdot \nabla f = 0. \tag{4}$$

The lead-free solder used in this study is SAC 305, with the compositions of 96.5% tin, 3% silver and 0.5% copper [10]. At the room temperature, SAC 305 solder is a solid, and it liquified after reaching its melting temperature. The molten solder binds the substrate and component lead after cooling phase. The surface area covered by the solder determines the strength of the solder joint. Thus, in melting phase, wetting of the solder to solder pad and lead component determine the reliability of the solder assembly. The term wetting commonly described as displacement of a solid-air interface with a solid-liquid interface [11]. The forces in equilibrium at a solid–liquid boundary is commonly described by the Young's equation

$$\gamma_{\mathrm{SG}} = \gamma_{\mathrm{LS}} + \gamma_{\mathrm{LG}} \cos\theta, \tag{5}$$

where γ_{SG}, γ_{LS} and γ_{LG} denote the interfacial surface energy between solid -vapor, solid-liquid and liquid-vapor respectively, and θ is the equilibrium contact angle [12]. To depict the surface interfacial effect and simulate the wall adhesion in the current simulation, the surface tension force and continuum surface stress settings were selected. The surface tension between SAC solder and air is set at 0.5 N/m [13]. The shear condition at solder pad and lead component boundary layer was set as no slip with the contact angle is set at 45°, indicating proper wetting.

The geometrical model was created with similar scale to the actual parts of the pin to hole (PTH) soldering assembly as depicted in Figure 1. The dimensions of PTH were based on IPC-2222 and IPC-2221 standards [14]. Using Level A of the standards, the lead diameter, hole diameter and outer diameter of solder pad are 0.8 mm, 1.0 mm and 1.5 mm respectively. Tetrahedral mesh was applied on the numerical model as shown in Figure 1. The mesh sizing was optimized upon taking account of both accuracy and computational time [15].

General boundary conditions (BC) used in current simulations are set using Fluid Volume Method (FVM) and Energy equation enabled, two phases of fluid material, air and solder is used. Heat source was set to 630 K to radiate heat on the top of solder pad and lead. A patched region for solder phase was created in close proximity of lead with sphere shape for uniform body forces. The sphere volume is decided by radius of the sphere where 0.6 mm is used. Pressure outlet is determined at fluid external boundary with pressure equal to atmospheric.

Heat source located above the solder pad is used to mimic the heat radiated from laser beam. Circular profile with same diameter of solder pad outer diameter is used to create radial heating distribution. The heat is set to 642 K constantly throughout the transient process. Heat radiated from this heat source will be absorbed on top of solder pad, lead, and solder. By conduction, the heat will distribute to all of these parts evenly at the end of simulation.

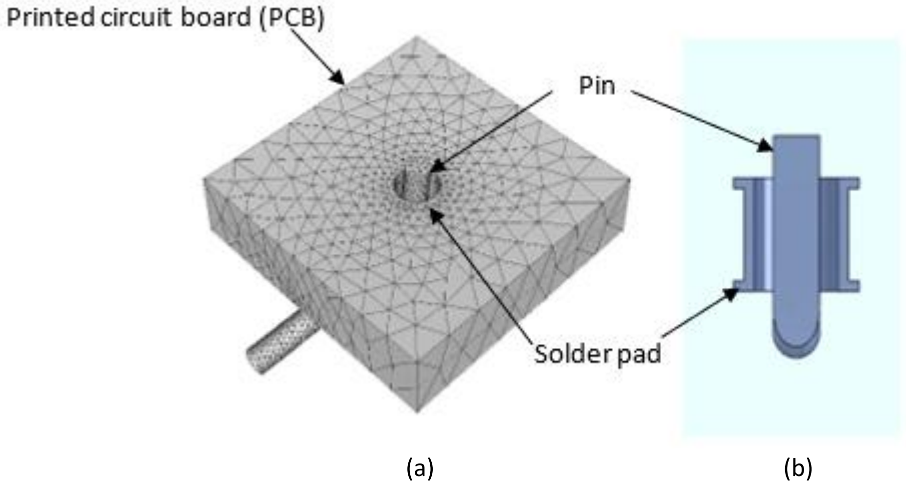

Fig. 1. (a) Meshed structural domain and (b) fluid domain

Using multiphase model, volume of fluid (FVM) is utilized to model the lead-free solder wetting process. In this case, SAC305 physical specification was used as shown in Table 1 as phase two parameter guide. The time step size used in current simulation is set at 0.1 s and the end time is 1.8 s. These settings were made consistent to the similar practice in industrial application. The solver used to solve coupling of both pressure and velocity in this model is Semi-Implicit Model (SIMPLE) algorithm scheme. This solver is used to obtain high accuracy result [13,16].

Table 1
Material properties of SAC305 solder [13]

Material properties	SAC 305 solder
Density	7500 kg/m^3
Viscosity	0.0022 Pa-s
Specific heat capacity	230 J kg˚K
Thermal conductivity	58 W m/K
Standard state enthalpy	0.04 J/mol

In order to facilitate heat conduction and radiation in the simulation model, physical surfaces of the model are assigned to respective material as shown in Figure 2. The physical and thermal properties of copper and FR4 composite were given in Table 2.

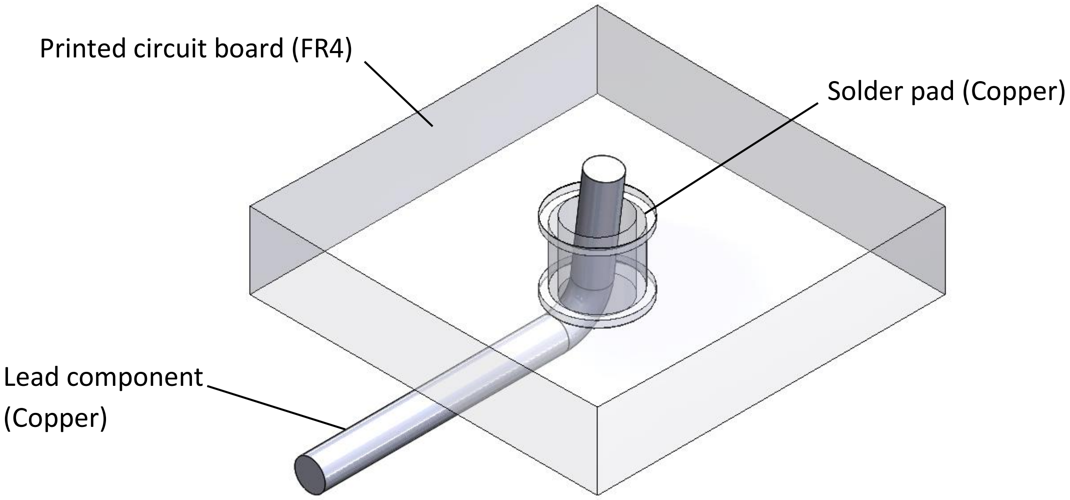

Fig. 2. Materials assignment to the solder and pin region

Table 2
Material properties of copper and FR4 composite for the solder pan and PCB respectively [14]

Properties	Copper	FR4 Composite
Density (kg/m^3)	8978	1700
Specific heat (J/kg-K)	381	920
Thermal conductivity (W/m-K)	387.6	0.2

The experiment is conducted in industrial environment using industrial grade laser soldering machine. The laser soldering system composed of laser diode, fiber optic module, focusing optics, computer vision module with camera, illuminator and motion module, the X-Y positioning platform with servo control system as shown in Figure 3 [17]

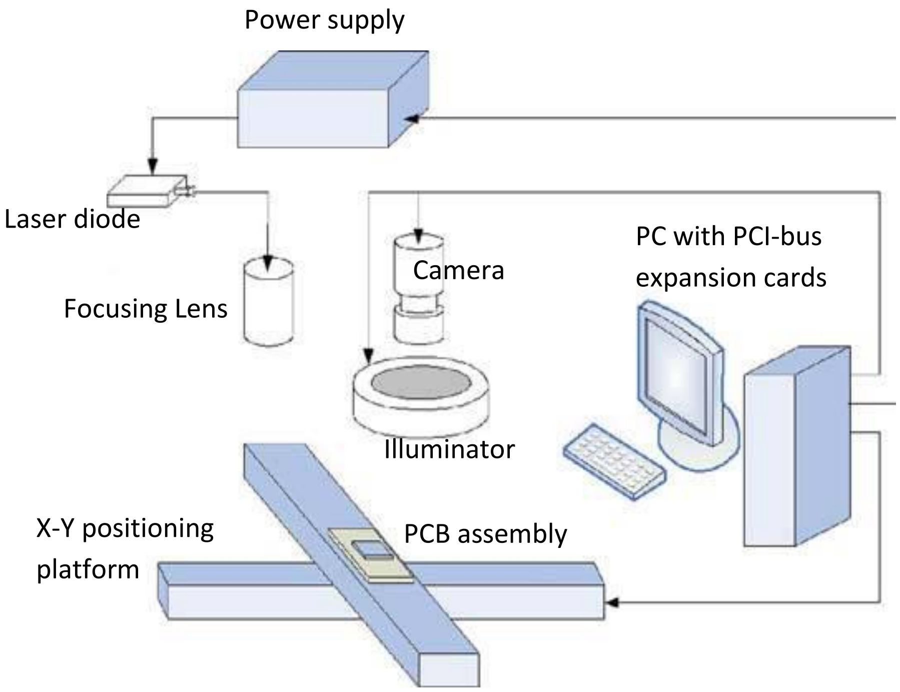

Fig. 3. Block diagram of laser soldering system

The heating temperature is set at 640 K. The solder region is pre-heated before the solder wire is feed onto the solder region. After the set temperature was meet, solder wire was feed onto the solder region and laser beam is introduced. The heating process then runs for 1.8 s to reflow the solder properly and completing wetting process between solder pad and lead component of PTH. Figure 4 shows the laser soldering process as configured by Japan Unix [18].

Fig. 4. Sequences of laser soldering process

3. Results and Discussion

Figure 5 compared the numerical simulated volume fraction of SAC305 solder with the experimental cross-section. In the simulation, lead of the component was tilted by 2° to mimic real condition based on the experiment. Generally, both numerical and experimental solder cross-sections are qualitatively comparable. The quantitative comparison on the numerical and experimental contact angles of the solder fillet located at the point A (refers Figure 5) was presented in Table 3, with the values of contact angle measured using an image processing tool. The absolute difference between numerical and experimental contact angle is 2°, which inferred that both the numerical and experimental solder fillet profiles are similar.

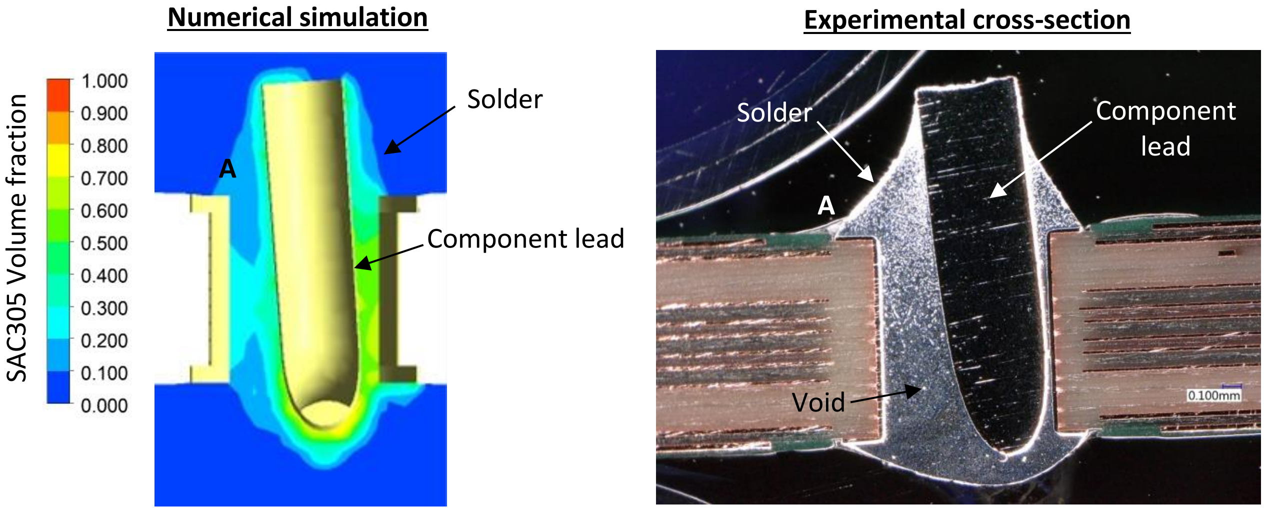

Fig. 5. Comparison between numerical simulated solder profile with the experimental cross-section

Table 3
Quantitative comparison on the numerical and experimental contact angles for the corresponding solder fillets located at the point A

Contact angle (°)		Discrepancy (%)
Numerical simulation	Experiment	
 X: 2.888 Y: 1.804 W: H: A: 60.7° L1: 0.094 L2: 0.067 60.7	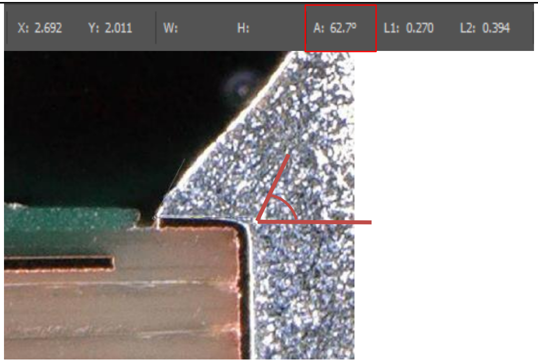 X: 2.692 Y: 2.011 W: H: A: 62.7° L1: 0.270 L2: 0.394 62.7	3.12

The regions marked with low solder volume fraction in numerical contours are constitutes to lower wetting ability, in which favours the void occurrent [19]. From Figure 5, the solder filled entirely the compartment space between the component lead and solder pad. The high volume fraction is between the most shortest distance between the two surfaces. This is because the flow velocity of solder is higher in the narrow region, in accordance to the continuity equation on the conservation of mass flow rate. As a result, the solder filled the narrow area faster and greatly reduce the tendency of void formation. This can be seen in experiment result where void formation is at the position where the lead component and solder pad distance is high.

Table 4 presents the numerically simulated flow mechanisms of SAC305 solder during the laser soldering process of PTH assembly. It can be seen that the solder upon being melted by the laser beam, it flows downward along the pin surface and filling the hole. The exceess solder then exited the hole and encapsulate the bottom section of pin. The solder took about 0.3 s to reach the bottom-most of the pin, and another 0.4 s to fully cover both the hole and pin, making the whole process lasts for 0.7 s.

Figure 6 shows the cross-sectional temperature distribution of the simulated laser soldering process. The high temperature zone is caused by radiation from heat source acting as the laser beam and conducted by solder pad, lead, and solder. At the end of transient simulation process, most of the solder region reached temperature of 642.31 K.

Fig. 6. Temperature distribution of simulated laser soldering process

Table 4
Transient evolutions of molten SAC 305 solder during the laser soldering process of PTH

Time (s)	Volume fraction of SAC305 Solder	Legend
0.3	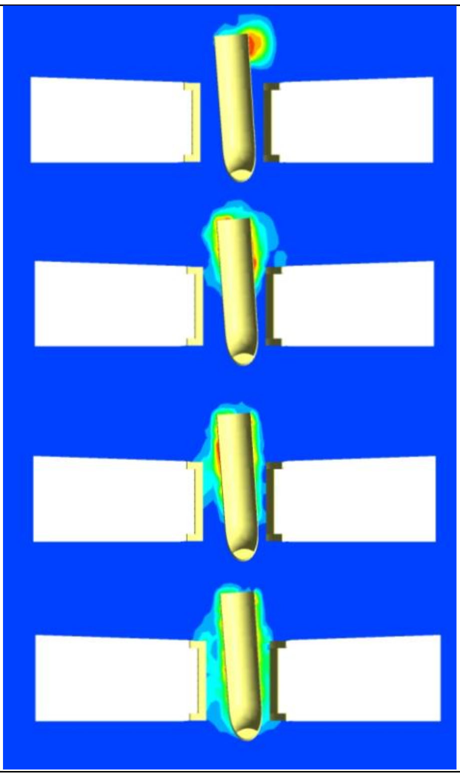	Volume fraction of SAC305 Solder 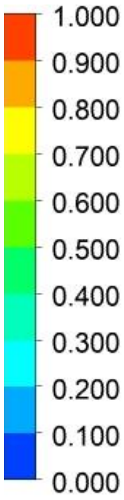
0.4		
0.5		
0.6		

0.7	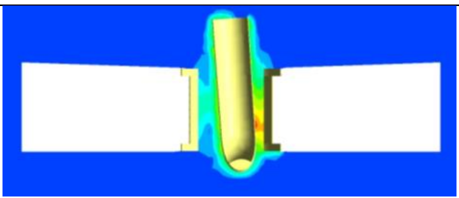
0.8	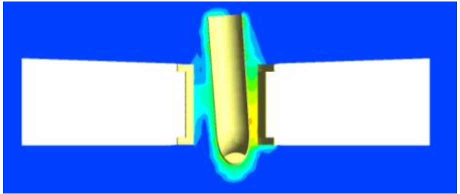
0.9	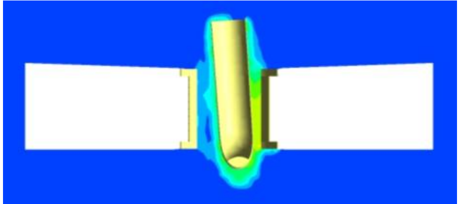
1.0	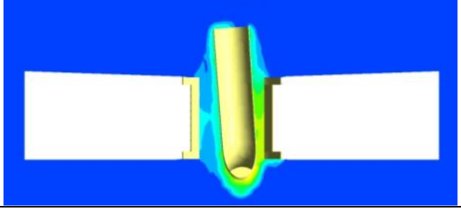

4. Conclusions

This paper had presented the numerical simulation of a laser soldering process on pin to hole (PTH) assembly, using the commercially available finite volume method (FVM) based software, ANSYS Fluent. The three-dimensional numerical model of laser soldering region was generated according to IPC standard and its free-surface model is generated using VOF method. The simulation result is then compared to experimental data. Both the numerical and experimental findings show great consensus, in which both solder fillet cross-sections are quantitative comparable. Further qualitative comparison on the contact angles gives a discrepancy of 2° or 3.12%, thus affirming the validity of numerical model. The transient evolution of solder flow during the process was presented, and at the present configurations, the solder took about 0.3 s to flow till the end of pin. Meanwhile, it took additional 0.4 s to fully fill the hole and cover the pin, making the laser soldering process took a total of 0.7 s. It was conjectured that the flow time was dependent on the rheology characteristics of solder, the dimensions of PTH and the thermal configurations of laser soldering process, in which these are variables to be optimized in future works. The current proposed numerical approach had enabled the modelling of laser soldering process, which provided useful insights for the future parametric optimization and process enhancement studies.

Acknowledgment

This work was partly supported by the following grants: Fundamental Research Grant Scheme (FRGS) (Grant No. 203/PMEKANIK/6071428) and Research University (RU) (Grant No. 8014071).

References

[1] Oppert, T., G. Azdasht, E. Zakel, and T. Teutsch. "Laser assisted soldering and Flip-Chip attach for 3-D packaging." In *2006 Thirty-First IEEE/CPMT International Electronics Manufacturing Technology Symposium*, pp. 86-86. IEEE, 2006. https://doi.org/10.1109/IEMT.2006.4456437

[2] Stella, Ezeonu. *Laser Soldering*. Materials Science - Advanced Topics, 2013. https://doi.org/10.5772/51527

[3] Nabila, T. J., S. R. A. Idris, and M. Ishak. "Optimization on laser soldering parameters onto lead-free solder joint." In IOP Conference Series: Materials Science and Engineering, vol. 238, no. 1, p. 012011. IOP Publishing, 2017. Nabila, T. J., S. R. A. Idris, and M. Ishak. "Optimization on laser soldering parameters onto lead-free solder joint." In *IOP Conference Series: Materials Science and Engineering*, vol. 238, no. 1, p. 012011. IOP Publishing, 2017. https://doi.org/10.1088/1757-899X/238/1/012011

[4] Baylakoglu, I., S. Hamarat, H. Gokmen, and E. Meric. "Case study for high volume lead-free wave soldering process with environmental benefits." In *Proceedings of the 2005 IEEE International Symposium on Electronics and the Environment*, 2005., pp. 102-106. IEEE, 2005.

[5] Ogbomo, Osarumen O., Emeka H. Amalu, N. N. Ekere, and P. O. Olagbegi. "Effect of coefficient of thermal expansion (CTE) mismatch of solder joint materials in photovoltaic (PV) modules operating in elevated temperature climate on the joint's damage." *Procedia Manufacturing* 11 (2017): 1145-1152. https://doi.org/10.1016/j.promfg.2017.07.236

[6] Dare, Ademola A., and Moses O. Petinrin. "Modelling of natural convection along isothermal plates and in channels using diffusion velocity method." *Maejo International Journal of Science and Technology* 4, no. 1 (2010): 43-52.

[7] Akay, Hasan U., Yan Liu, and Mostafa Rassaian. "Simplification of finite element models for thermal fatigue life prediction of PBGA packages." *Journal of Electronic Packaging* 125, no. 3 (2003): 347-353. https://doi.org/10.1115/1.1569956

[8] Ng, Fei Chong, Aizat Abas, and Mohd Zulkifly Abdullah. "Effect of solder bump shapes on underfill flow in flip-chip encapsulation using analytical, numerical and PIV experimental approaches." *Microelectronics Reliability* 81 (2018): 41-63. https://doi.org/10.1016/j.microrel.2017.12.025

[9] Ng, Fei Chong, and Mohamad Aizat Abas. "Underfill flow in flip-chip encapsulation process: a review." *Journal of Electronic Packaging* 144, no. 1 (2022). https://doi.org/10.1115/1.4050697

[10] Hlinka, József, Zsolt Fogarassy, Ágnes Cziráki, and Zoltán Weltsch. "Wetting properties, recrystallization phenomena and interfacial reactions between laser treated Cu substrate and SAC305 solder." *Applied Surface Science* 501 (2020): 144127. https://doi.org/10.1016/j.apsusc.2019.144127

[11] Zhong, W. "Surface tension, wetting and wicking." *ed. North America: Woodhead Publishing Limited* (2006): 136-153. https://doi.org/10.1533/9781845692261.1.136

[12] Ng, Fei Chong, and Mohamad Aizat Abas. "Surface energetic-based analytical filling time model for flip-chip underfill process." *Soldering & Surface Mount Technology* 33, no. 5 (2021): 281-290. https://doi.org/10.1108/SSMT-10-2020-0042

[13] Haslinda, M. S., Aizat Abas, F. Che Ani, Azman Jalar, A. A. Saad, and Mohd Zulkifly Abdullah. "Discrete phase method particle simulation of ultra-fine package assembly with SAC305-TiO_2 nano-reinforced lead free solder at different weighted percentages." *Microelectronics Reliability* 79 (2017): 336-351. https://doi.org/10.1016/j.microrel.2017.07.054

[14] Association Connecting Electronic Industries (IPC). Illinois, February 1998. https://www.ipc.org/TOC/IPC-2221A.pdf.

[15] Ng, Fei Chong, Aizat Abas, Ismail Abustan, Z. Mohd Remy Rozainy, M. Z. Abdullah, and Sharon Melissa Kon. "Effect of the gap height of radial gate on the volumetric flow rate in dam." In *IOP Conference Series: Materials Science and Engineering*, vol. 370, no. 1, p. 012062. IOP Publishing, 2018. https://doi.org/10.1088/1757-899X/370/1/012062

[16] Ng, Fei Chong, Mohamad Aizat Abas, and Mohd Zulkifly Abdullah. "Filling efficiency of flip-chip underfill encapsulation process." *Soldering & Surface Mount Technology* 32, no. 1 (2020): 10-18. https://doi.org/10.1108/SSMT-07-2019-0026

[17] Xiong, Zhenhua, Xinjue Zou, Yulin Wang, and Han Ding. "Development and error compensation of laser soldering system." *Assembly Automation* 30, no. 3 (2010): 213-220. https://doi.org/10.1108/01445151011061109

[18] Japan Unix. "Laser soldering method & theory." *JAPAN UNIX*. Accessed June 24, 2021. https://www.japanunix.com/en/method/laser/.

[19] Ng, Fei Chong, Mohd Hafiz Zawawi, and Mohamad Aizat Abas. "Spatial analysis of underfill flow in flip-chip encapsulation." *Soldering & Surface Mount Technology* 33, no. 2 (2020): 112-127. https://doi.org/10.1108/SSMT-05-2020-0017